Journal of Advanced Zoology

ISSN: 0253-7214

Volume ***45 Special*** *Issue* ***02 Year 2023*** *Page* ***1240:1263***

DEVELOPMENT AND EVALUATION OF DOXORUBICIN ANCHORED PLGA NANOPARTICLES AGAINST BREAST CANCER

Tarun Kumar [1], Vinay Pandit [2], Ranjit Singh [1]

1. Research Scholar, Adarsh Vijendra Institute of Pharmaceutical Sciences (AVIPS), Shobhit University Gangoh (UP)
2. Professor & Head, Department of Pharmaceutics, Laureate Institute of Pharmacy Kathog (HP)
3. Vice Chancellor, Shobhit University Gangoh (UP)

Mail id: tarunsharmaguleri@gmail.com

Graphical Abstract

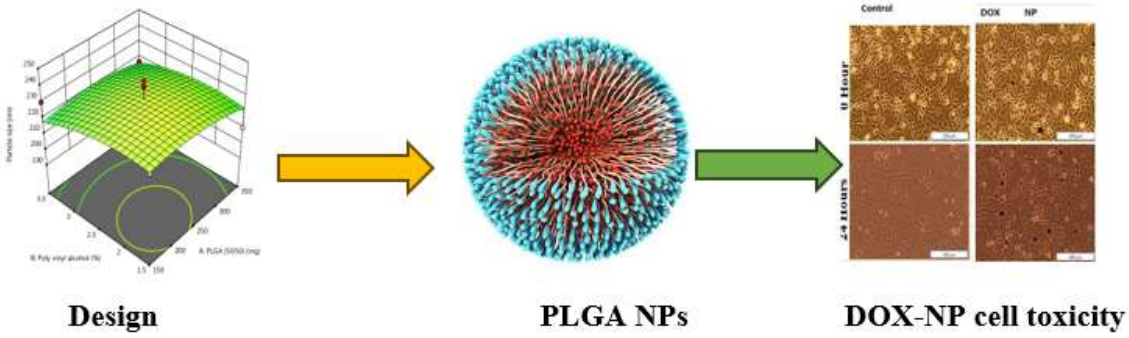

Article History
Received: 11 February 2023
Revised: 21 August 2023
Accepted: 05 October 2023

Abstract

The objective of this work was to design and develop Poly (D, L-Lactide-co-glycolide) (PLGA) nanoparticles (NPs) of Doxorubicin for the effective treatment of breast cancer. The nanoparticles (NPs) were optimized by applying a Box-Behnken design (BBD) using Design-Expert® Software and prepared using the double emulsification and precipitation method. Three independent factors such as PLGA 50:50 (A), PVA (B), stirring speed (C) were considered. Three dependent responses included entrapment efficiency (Response 1), particle size (Response 2) and Doxorubicin release at 10th hour (Response 3). ATR and DSC studies indicated compatibility between the drug and polymer.

The morphological studies performed by SEM showed uniform and spherical shaped discrete particles with smooth surface and in a size range of 282.6 nm. X-ray diffraction was performed to confirm the crystalline nature of the drug after encapsulation. The NPs exhibited a zeta potential of 21.6 mV. *In vitro* release studies showed a drug release up to 10 hrs. The release kinetics study indicated first order kinetics while the release mechanism followed Higuchi model. The cell viability was found to be more than 80% after incubation with the DOX NPs for 24 h up to a concentration of 80 μg/ml. The DOX NPs treated MCF-7 displayed intrinsic cell damage and cell shrinkage as compared to the control group. It may be concluded from the present investigation that PLGA NPs bearing doxorubicin can effectively treat the breast cancer.

Keywords: Nanoparticles, PLGA, Doxorubicin, breast cancer, design of experiment, target delivery

Introduction

Doxorubicin hydrochloride is used widely in ovarian, breast and lung cancer as well as malignant lymphoma [1, 2] however, the cardiotoxicity associated side effect limits its long term use for such clinical purposes [3, 4]. The additional P-glycoprotein (P-gp) as well as multidrug-resistance-associated protein-1 (MRP1) mediated efflux, makes the tumor cells less sensitive towards DOX [5]. The disadvantages such as cardiac toxicity and short half-life [6, 7], poor solubility, lack of availability of oral dosage form (most invasive, cost effective and painless route), instability of drugs in gastric conditions and hepatic first pass effects hinder the use of most drugs [8].

To address these gaps and improve the oral efficacy of drugs, various approaches in the form of polymer prodrugs [9], polymer conjugates [10], liposomes [11], solid lipid NPs [12] and polymeric nanoparticles (NPs) [13], have been evaluated.

Recently, nanoscale drug delivery systems have been gaining in popularity. Entrapping drugs in nanocarriers can overcome the above impediments by modifying drug bio distribution and controlling drug release [14].

PLGA is approved by the Food and Drug Administration and the European Medicines Agency as a part of various drug delivery systems for human applications. Several drugs

(including dexamethasone, 5-fluorouracil and paclitaxel) have been successfully incorporated into PLGA.

Owing to good biocompatibility properties, biodegradability, nontoxicity, nonimmunogenicity and sustained release properties, PLGA NPs have been widely used as drug delivery carriers for anticancer drugs [15].

Materials and Experimental Methods

Materials

The drug (Doxorubicin) was obtained as a gift sample from Neon Laboratory Pvt. Ltd. Mumbai. Poly (lactic-co-glycolic) Acid (PLGA) (50: 50), ethyl acetate, and polyvinyl alcohol (PVA) were procured from Sigma Aldrich Company. India. The human breast cancer cell line (MCF-7; ATCC HTB-22) was obtained from The American Type Culture Collection (ATCC). The cell culture growth medium Dulbecco's modified Eagle's medium (DMEM; D5796) was received from Sigma-Aldrich. The breast cancer cells were maintained in Dulbecco's Modified Eagle's Medium (DMEM) supplemented with 10% fetal bovine serum (FBS, 10499− 044; Gibco), 1% penicillin−streptomycin (P4333), and 1% amphotericin B (A2943) in 85% humidified atmosphere at 37°C and 5% CO_2. CytoTox 96 non-radioactive cell toxicity assay was obtained from Promega Corporation (Madison, WI, USA).

Melting point (MP) determination

The capillary method was done by placing the sample in a capillary tube by heating the sample until the melting point was achieved and thus, the melting point was recorded. [16]

Solubility determination

The solubility of the drug in various solvents such as 0.1 N hydrochloric acid, distilled water, phosphate buffer 6.8, 7.4, methanol, ethanol and dimethyl sulfoxide (DMSO) was determined by saturated solubility method. In this method excess of the drug was added in a total of 2ml of each of the above-mentioned solvents and this mixture was shaken on rotary flask shaker at room temperature for 24 hr. [17]. The filtered supernatants were further diluted and analyzed by a spectrophotometer at 475 nm for the drug content. Thus the solubility of Doxorubicin in the respective solvent was calculated. All experiments were carried out in triplicate.

Preparation of PLGA nanoparticles

Fifty milligram of the drug was dissolved in a 1.0 ml of DMSO. In another beaker specified amount of PLGA dissolved in 4 ml of Dichloromethane (DCM). The drug solution was poured to a precooled (10°C) PLGA solution and subjected to sonication in a probe sonicator (UAI-PS20khz-900W, Ultra Autosonic, India) for 10 minutes at 6% amplitude [18]. This

procedure resulted in a w/o emulsion. To this emulsion, a specified amount of PVA solution was added; and further sonicated for 10 minutes under an ice bath after covering with an aluminum foil to develop double emulsion. Finally, 30 ml of PVA (1% w/v) solution was added under magnetic stirring (1000 RPM, Remi stirrer, Mumbai, India) to evaporate excess DCM and DMSO. The precipitated nanosuspension was further washed with distilled water thrice (Bench top centrifuger, Sigma 3-30 KS, Germany) for 15 minutes and the excess PVA was removed by decantation. The resulted preparation was lyophilized (BK FD10, Biobase, China) for 24h at -80°C and stored at 4°C till further use.

Formulations suggested by Box-Behnken design (BBD)

A five-level three-factor Box-Behnken experimental design was used in the present study to assess the effects of selected independent variables on the responses. Four independent factors such as sodium PLGA 50:50 (A), PVA (B), stirring speed (C) were taken (**Table 1**). The responses recorded in the experiment include drug release at 10 hours, EE, particle size [19]. The *polynomial equation* was used for mathematical fitting and analysis. The optimized formula was solved by graphical optimization technique along using a numerical method at the confidence interval value of alpha 0.05.

Table 1: Formulation optimization using DoE

	Factor 1	Factor 2	Factor 3	Response 1	Response 2	Response 3
Run	A:PLGA (50:50)	B:Poly vinyl alcohol	C:Stirring speed	EE	Particle size	% Doxorubicin release at 10 h
	mg	%	RPM	%	nm	%
1	250	2.5	3000	47	220	88.81
2	150	2.5	4000	58	198	90.17
3	250	3.5	2000	52	201	81.39
4	350	2.5	2000	72	221	83.18
5	150	2.5	2000	66	216	91.98
6	150	3.5	3000	68	230	85.18
7	350	1.5	3000	79	210	82.19
8	250	2.5	3000	58	238	79.91
9	250	2.5	3000	47	241	89.18

10	250	3.5	4000	58	198	66.74
11	250	2.5	3000	46	215	80.17
12	250	2.5	3000	53	237	71.28
13	150	1.5	3000	59	228	99.85
14	350	3.5	3000	66	217	61.76
15	350	2.5	4000	71	209	70.08
16	250	1.5	4000	51	197	71.28
17	250	1.5	2000	53	245	82.61

Characterization of the nanoparticles

Drug loading (DL)

In a 100 mL volumetric flask, an accurately weighed quantity of nanoparticles (equivalent amount of 50 mg of Doxorubicin) was placed, and a minimum amount of ethanol was added and thoroughly mixed. The dispersion was sonicated for about 10 minutes (Ultrasonicator, CPX3800-E, Branson). Phosphate buffer pH of 6.8 was added to the resultant mixture and the volume was adjusted to the desired level [20]. The dispersion was bath sonicated for an additional 10 minutes, until it became transparent. The resulting mixture was subsequently filtered using a 0.45 m pore size Whatman membrane filter. To quantify Doxorubicin content, the filtrate was analyzed with a UV-Visible spectrophotometer (Shimadzu UV-1800, Japan) at 475 nm. Using the following formula, the percent drug loading (DL) was estimated.

$$\text{DL}\ (\%) = \frac{\text{Doxorubicin content in nanoparticle}}{\text{Total weight of nanoparticle}} \text{ x } 100 \quad \ldots\ldots\ldots \text{(Equation 1)}$$

***In-vitro* drug release**

In vitro drug release from the nanoparticles was performed by diffusion technique using Franz-diffusion cell. The cellophane membrane was cut into equal pieces (6 cm×2.5 cm) and soaked into distilled water for 6 h before use. The release studies were carried out in 10 ml of phosphate buffer saline pH 6.8 maintained at 37±0.5° using a magnetic stirrer (IKA Auto Temp Regulator, Germany). About 2 ml of nanoparticles suspension was placed in receptor

compartment. An aliquot of 1 ml was withdrawn at the regular interval and replaced with same volume of fresh buffer. The aliquots were diluted with fresh medium. [21,22]. The amount of the drug diffused through the membrane was measured by using U.V. spectrophotometer at the wavelength 475 nm against phosphate buffer (pH 6.8) as the blank.

Attenuated total reflection (**ATR) study**

The sampling technique ATR (Attenuated total reflection) was used in conjunction with infrared spectroscopy which examines the sample directly in solid or liquid state without further preparation. ATR spectroscopy was used for monitoring the polymer composition. The study was carried out by ***Bruker Opus 7.0, Germany.***

Differential Scanning Calorimetry (DSC) study

The thermal analysis apparatus DSC was used to show how physical properties of a sample change along with temperature against time [24]. The study was carried out by **DSC-60, Shimadzu, USA.**

X Ray Diffraction (XRD) study

A non-destructive test technique was used to examine the crystalline material's structure known as X-Ray Diffraction. The use of XRD analysis was to identify the crystalline phases that comprise material information about its chemical composition [25]. XRD study was carried out by ARL EQUINOX 100, Thermo Scientific, India.

Surface morphology, Particle size and zeta potential of optimized formulation

The morphology of the optimized Doxorubicin nanoparticles was studied using scanning electron microscope [26]. The sample was attached to the slab surface with double sided adhesive tape and the scanning electron microscope (S3700N-Hitachi, Japan) Photomicrographs were taken at different magnifications [27]. Similarly, the nanoparticles evaluated for particle size and poly dispersity index value using the scattering light intensity technique (Malvern Zetasizer, ATA Scientific, USA).

In vitro cell toxicity

Cell Toxicity (LDH Assay)

The CytoTox96 assay kit was used to examine the cell-toxicity of DOX nanoparticles. LDH, a stable cytosolic enzyme produced during cell lysis, is quantified in the CytoTox96 assay. LDH is an enzyme that catalysis the inter conversion of pyruvate and lactate [28]. Fifty microliters of the control and test samples were put to a 96-well plate, along with the same

amount of the LDH reagent, and the wells were incubated in the dark for 30 minutes at room temperature. A multilabel counter (Perkin Elmer, VICTOR3 Multilabel Plate Reader, 1420) was used to measure the amount of LDH released using a spectrophotometer at 490 nm. Furthermore, the IC_{50} concentration was analyzed using the following equation

$$\text{Cell toxicity (\%)} = \frac{\text{OD of the experimental LDH release}}{\text{OD of the maximum LDH release}} \times 100$$

Cell Morphological Analysis. The cell morphology changes in 0 h- and 24 h-treated groups were visualized using a CKX41 inverted microscope (Olympus, Wirsam) [29]. The cell morphology changes were captured at different time hours (0 and 24 h).

In Vitro Cell Toxicity (Lactate Dehydrogenase Assay): When cells were destroyed, a stable cytosolic enzyme called lactate dehydrogenase (LDH) was produced. This enzyme might be utilized to assess the cell viability and toxicity of breast cancer cells [30].

Results and Discussion

Solubility studies in different solvents

The drug exhibited high solubility in organic solvent; maximum in DMSO followed by distilled water and 0.1N hydrochloric acid**.**

Table 2: Solubility of Doxorubicin in different solvents

Solvent	Solubility (mg/ml)
0.1N Hydrochloric Acid	3.71±1.1
Distill water	12.57±1.09
Phosphate buffer 6.8	2.98±0.71
Phosphate buffer 7.4	1.39±0.84
Methanol	0.97±0.01
Ethanol	0.58±0.08
DMSO	95.52±3.17

Drug loading (%)

It was observed that formulations loaded with high amount of PLGA (50:50) showed high drug loading. Formulation “F14” showed maximum drug loading at 71.34% followed by F4 and F15 with 68.11% and 65.55% of loading, respectively. The formulation with lesser amount of PLGA exhibited low drug loading as seen in “F13” which could entrap only

48.37% of the drug. This clearly indicates hydrophobic nature of PLGA facilitated high drug retention in the nanoparticles.

Table 3: Doxorubicin loading of different formulations

Run	Amount of the drug (mg)	Percent drug loading
F1	29.13	58.27±2.38
F2	25.90	51.81±1.15
F3	30.64	61.29±3.29
F4	34.05	68.11±2.07
F5	27.64	55.29±1.39
F6	29.52	59.04±1.02
F7	30.82	61.64±2.18
F8	28.92	57.85±3.31
F9	29.81	59.63±1.08
F10	27.19	54.38±2.28
F11	26.99	53.99±1.39
F12	29.58	59.17±3.08
F13	24.18	48.37±2.41
F14	35.67	71.34±1.17
F15	32.77	65.55±2.15
F16	24.59	49.18±3.07
F17	25.86	51.73±1.08

Similar behavior was noted from the nanoparticles with high amount of PVA which indicates that PVA developed a viscous layer barrier which trapped more amount of Doxorubicin in NPs. Finally, it can be concluded that, a suitable combination of PLGA and PVP can develop a NPs with good drug loading. The highest EE (79%) was noted in the formulation F7 which contains 350 mg of PLGA and 1.5% of PVA. Likewise, F4 exhibited 72% of drug loading which contains 350 mg of PLGA and 2.5% of PVA.

Model Validation

Effect on independent variables on Response 1- % EE

The polynomial equation plotted and the synergistic and antagonist variables affecting the responses were recorded. In Response 1, A, interaction term (AB) and Quadratic term A^2 are significant.

Response 1 [EE]=50.2+**4.625A**+0.25B-0.625C-**5.5AB**+1.75AC +2.0BC + **15.525A^2** + 2.0275B^2 +1.025C^2 ……. (2)

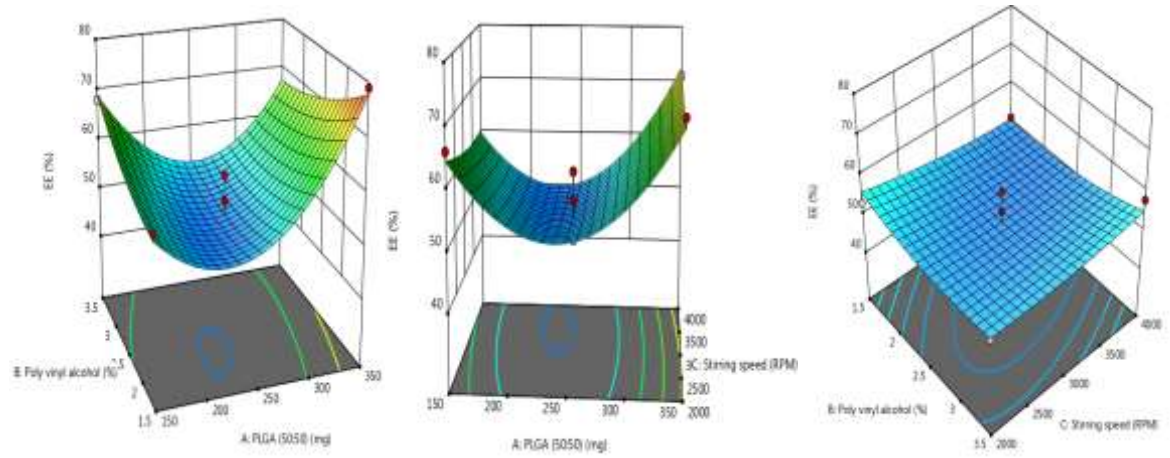

Figure 1: RSM curve of Response 1(EE)

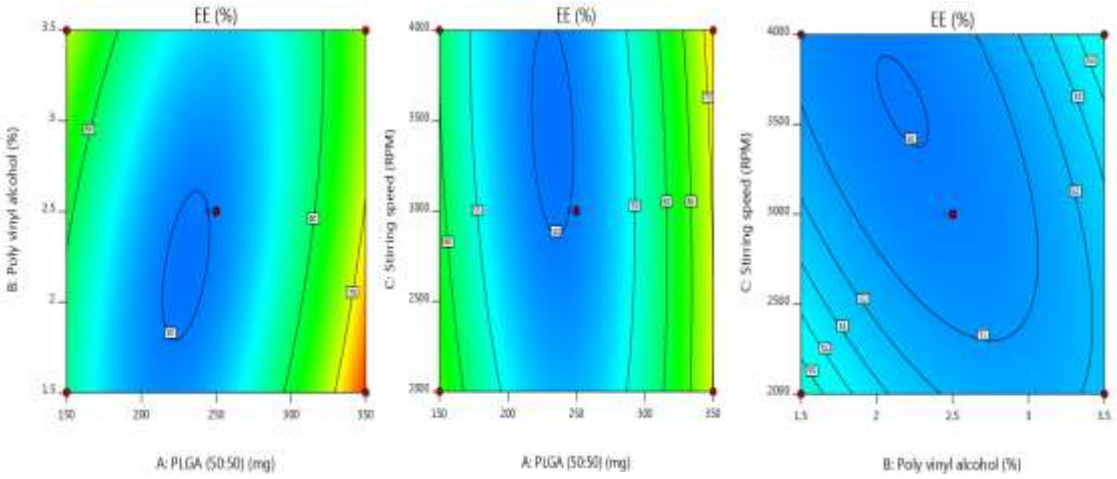

Figure 2: Contour plot of Response 1(EE)

Effect on independent variables on Response 2- Particle size

The polynomial equation plotted and the synergistic and antagonist variables affecting the responses were recorded.

Response 2 [Particle size] = 230-**1.875A**-4.25B-**10.125C**+1.25AB+1.5AC +11.25BC-4.1A^2-**4.85B^2**-15.1C^2…… (3)

In Response 2, A, C and Quadratic term B^2 are significant.

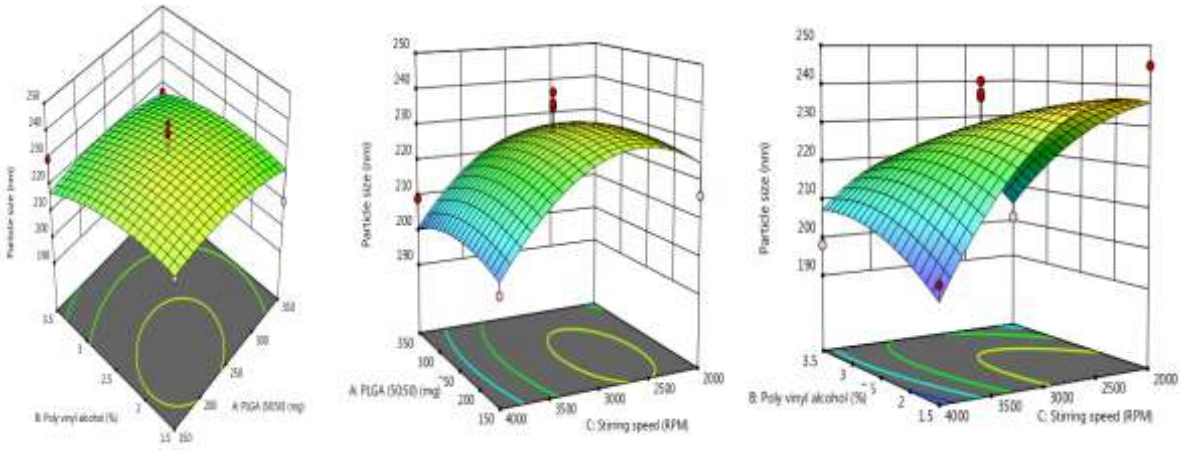

Figure 3: 3D simulation curve of Response 2(Particle size)

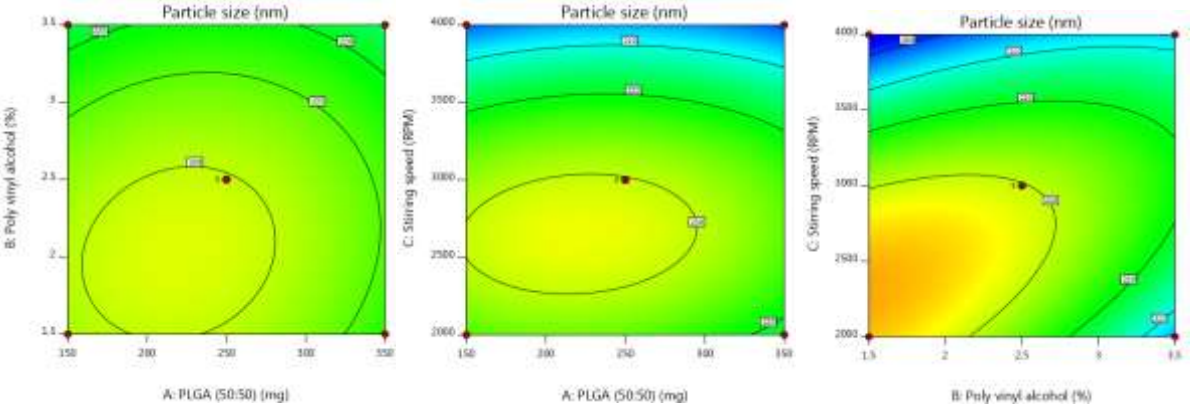

Figure 4: 2D Contour plot of Response 2(Particle size)

Effect on independent variables on Response 3- % Doxorubicin release at 10 h

The polynomial equation plotted and the synergistic and antagonist variables affecting the responses were recorded.

Response 3 [% Doxorubicin release at 10h] = 81.87-**8.74A**-5.10B-5.11C-1.44AB-**2.82AC** -0.83BC+4.36A^2-3.98B^2-2.37C^2……. (4)

In Response 3, A, and interaction term AC are significant.

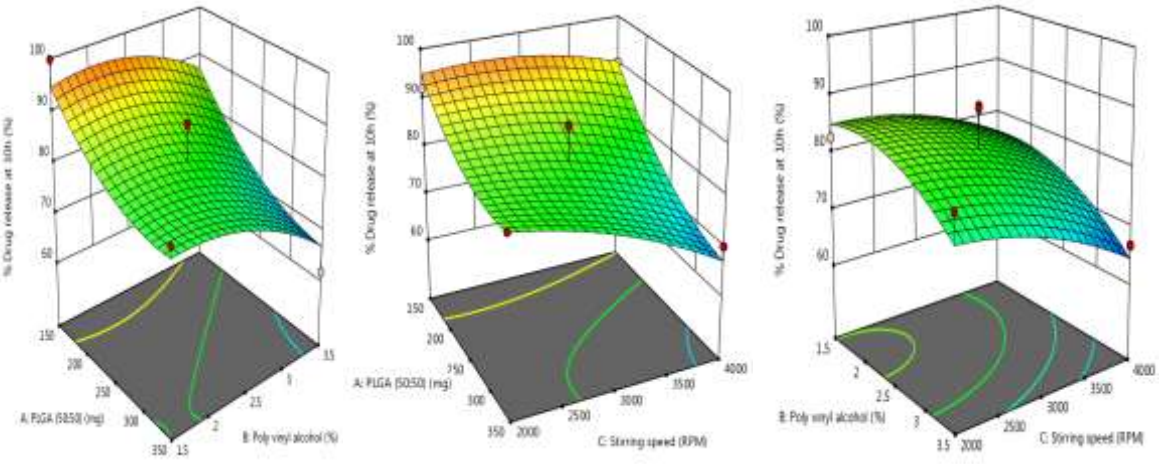

Figure 5: 3D simulation curve of Response 3(Doxorubicin Release at 10 h)

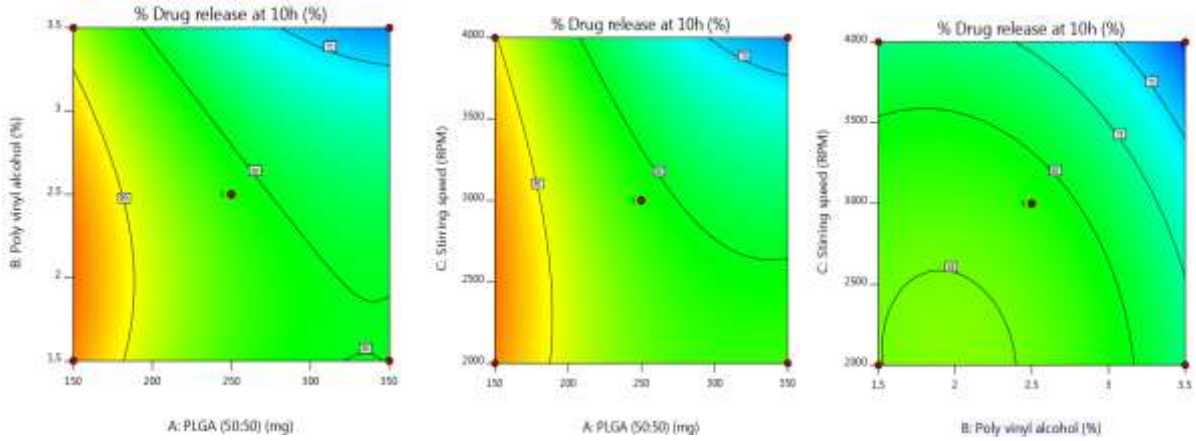

Figure 6: Contour plot of Response 3 (Doxorubicin release at 10h)

Optimization of study

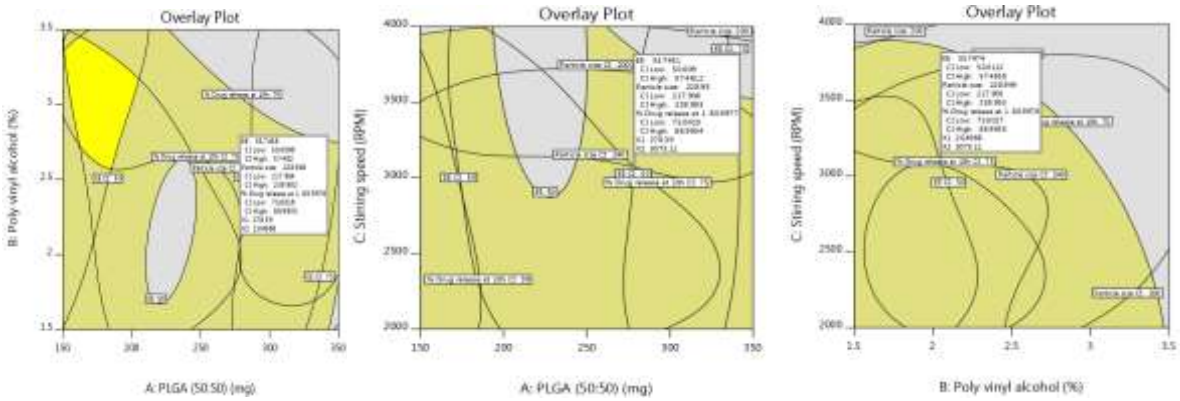

Figure 7: Overlay plot of region highlighting the optimized space and values

After generating the model polynomial equations, the process was optimized based on the relationship between the dependent and independent variables [31].

Table 4: Formulation optimization

Name	Level	Low Level	High Level	Std. Dev.	Coding
PLGA (50:50)	312.28	150.00	350.00	0.0000	Actual
Poly vinyl alcohol	2.07	1.50	3.50	0.0000	Actual
Stirring speed	3625.11	2000.00	4000.00	0.0000	Actual

The experimental parameters were optimized using the canonical analysis, which allows the compromise among various responses and searches for a combination of factor levels that jointly optimize a set of responses by satisfying the requirements for each response in the set. From the mathematical and graphical method of optimization; the best and optimized formulation was developed and the DoE space (Yellow colour region) is mentioned in Figure

7. Prior to the finding of optimized formulation, the target ranges (for responses) were fixed from the literature survey.

Table 5: Point prediction of optimized formulation

Response	Predicted Mean	Predicted Median	Observed	Std dev.	SE Mean
EE	64.33	64.33	67.15	4.48091	2.5894
Particle size	210.782	210.782	282.6	13.2452	7.65405
% Drug release at 10h	73.2519	73.2519	79.33	7.19103	4.1555

In-vitro drug release

The nanoparticles were subjected to in vitro drug release study. All the formulations could release a minimum 15% of drug within 30 minutes. The release was observed up to 10h, a few formulations released near to 100% of drug such as "F13" released 99.85%, the highest, while F14 released only 61.76%. A comparison was made between the formulations F4 and F5 whose composition differ in percentage of PLGA. F4 released only 83.18%; whereas F5 released 91.98%, suggesting that, the higher amount of PLGA delayed drug release.

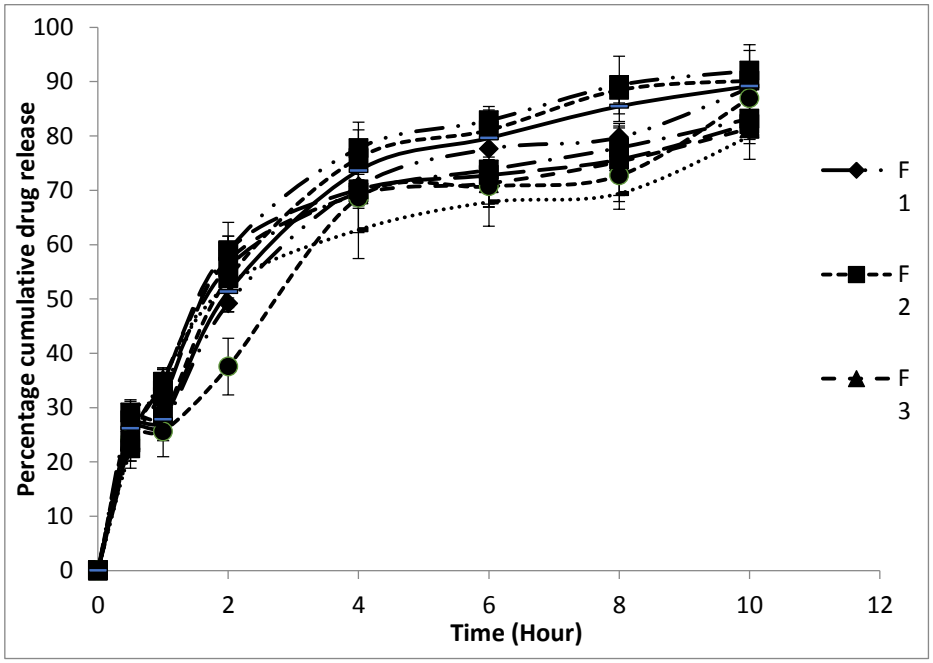

Figure 8: In vitro release profile of different formulations

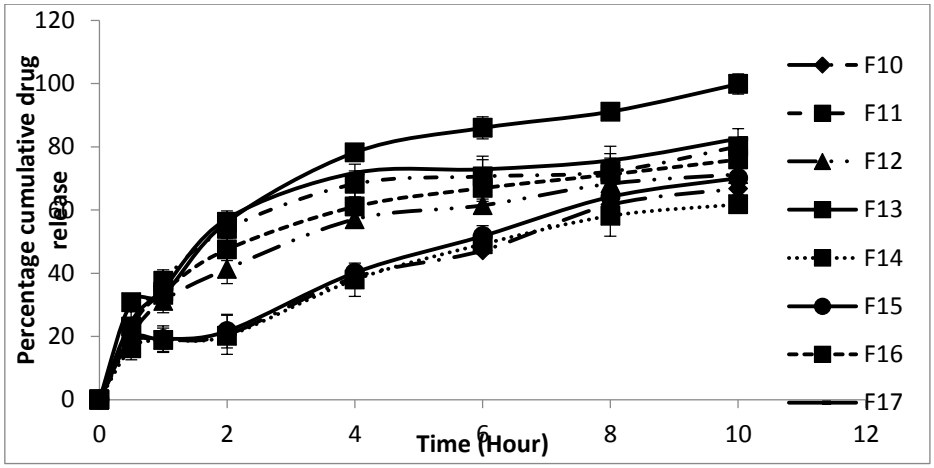

Figure 9: In vitro release profile of different formulations

It was noted that the formulations such as F4, F7, F14 and F15 containing 350 mg of PLGA, the highest amount could release comparatively lesser drug amounting to 83.18%, 82.19%, 61.76% and 70.08%, respectively. This is possibly due to the hydrophobic nature of PLGA, resulting in a barrier around the NPs which hindered the release. Similarly, it was noted that higher amount of PVA developed a highly viscous layer and retarded drug release. The pattern can be seen in "F10" which released 66.74% of the drug, while the formulation F6 released 85.18% of the drug. This indicated that both PLGA and PVA could delay the drug release in suitable combination. While developing NPs stirring speed was also fixed as one of the independent variables. The RPM was fixed from 2000 as minimum and 4000 as highest value. The higher RPM developed smaller NPs while lower RPM developed larger NPs as exhibited by the particle size analysis. It was observed that the size of NPs in the formulation F10 was 198 nm whereas in the formulations F17 and F4 the size was 245 nm and 221 nm, respectively. This indicates the effect of RPM on the dissolution pattern of NPs.

Table 6: Release kinetics study of the formulations

Formulation	Zero	First	Higuchi	Hixson-Crowell	Korsemeyer-Peppas	
					(R^2)	n
F1	0.839	0.936	0.966	0.910	0.808	0.245
F2	0.850	0.973	0.971	0.943	0.808	0.308
F3	0.748	0.863	0.931	0.827	0.753	0.291
F4	0.787	0.904	0.950	0.869	0.789	0.311
F5	0.823	0.968	0.964	0.930	0.791	0.421
F6	0.838	0.895	0.953	0.880	0.789	0.306

F7	0.741	0.853	0.925	0.819	0.752	0.179
F8	0.745	0.853	0.933	0.820	0.744	0.410
F9	0.853	0.967	0.973	0.937	0.814	0.284
F10	0.946	0.968	0.960	0.965	0.767	0.316
F11	0.737	0.843	0.927	0.911	0.742	0.319
F12	0.834	0.931	0.978	0.903	0.786	0.276
F13	0.841	0.983	0.974	0.950	0.790	0.299
F14	0.948	0.979	0.972	0.971	0.793	0.218
F15	0.951	0.976	0.963	0.973	0.775	0.338
F16	0.801	0.914	0.965	0.881	0.765	0.315
F17	0.744	0.851	0.928	0.819	0.751	0.228

The release kinetics study was done to ascertain the release models. It was observed that all the formulations followed first order kinetics as indicated by the R^2 value indicating the dependence of release on the concentration of the drug and polymer. The release mechanism was ascertained by Higuchi, Hixon-Crowell and Korsemeyer-Peppas models (Table 6) and it was noted that most of the formulations obeyed Higuchi model. This model describes the release of drugs from insoluble matrix as a square root of time dependent process. The study indicates that high amount of PLGA in the formulations resulted in hydrophobic nanoparticles and their release mechanism depended on surface area and change in diameter of the particle during the process of dissolution.

ATR study

A broad peak at 3563.03 cm^{-1} is due to O-H stretching. Similarly C-H stretching exhibited peak at 2920.29 and 2483.93 cm^{-1}. A prominent peak appeared at 1765.95 cm^{-1} developed by C=O stretching. Carbonyl C-O-C stretching developed peaks at 1165.34 and 1109.55 cm^{-1}. Characteristic C=C stretching peaks developed at 1407.32, 1523.79 and 1619.80 cm^{-1}.

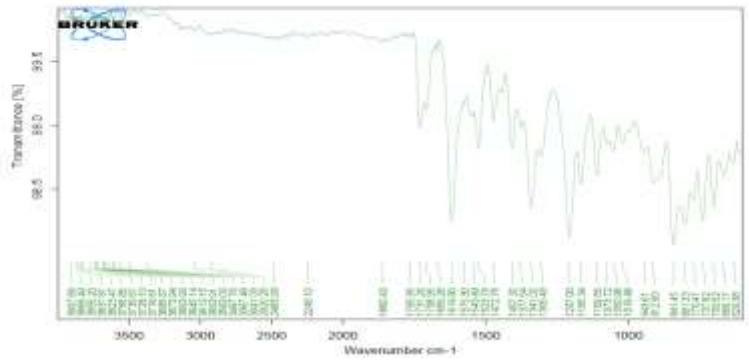

Figure 10: ATR spectra of Doxorubicin

Equal amount of drug and excipients taken in a clean and dry mortar pestle and triturated to get a physical mixture. The physical mixtures (Doxorubicin + PLGA; Doxorubicin + PVA) were subjected to ATR study for compatibility assessment.

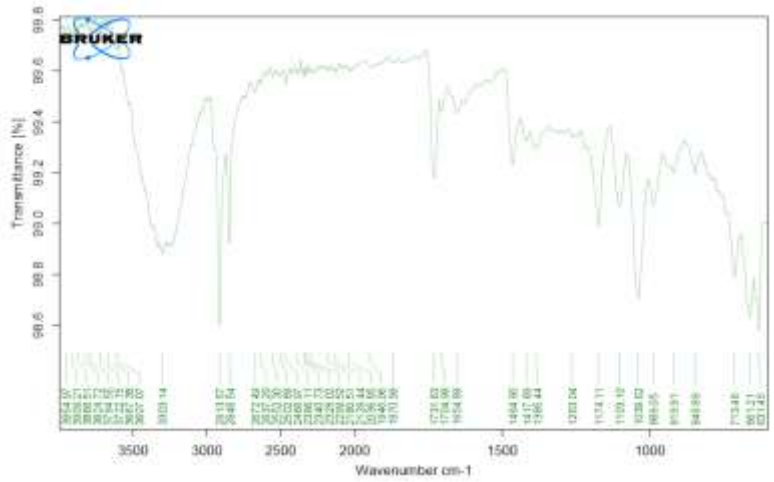

Figure 11: ATR spectrum of Doxorubicin+ PLGA

No significant changes in peak position were observed which indicate the compatibility of the drug with selected excipients.

In the optimized formulation, it was noticed that there was a small intensity peak at 3607.99 cm^{-1} that was contributed by N-H stretching. The O-H stretching resulted in a broad peak at 3286.46 cm^{-1}. In a similar fashion, the C-H stretching reached its maximum at 2926.27 cm^{-1}. At 1732.98 cm^{-1}, a prominent peak that had been produced via C=O stretching was observed. Both 1197.95 and 1263.13 cm^{-1} were found to be peak frequencies for carbonyl C-O-C stretching. C=C stretching peaks that are characteristic of the system formed at 1431.87, 1522.72, and 1693.91 cm^{-1}.

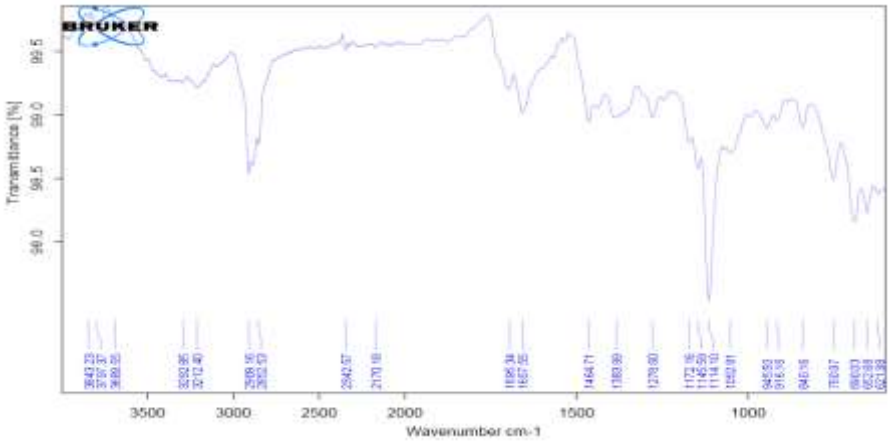

Figure 12: ATR spectrum of Doxorubicin + PVA

Summarily it was observed that all the major groups related to Doxorubicin are present in the optimized formulation indicating no interaction between the drug and excipients.

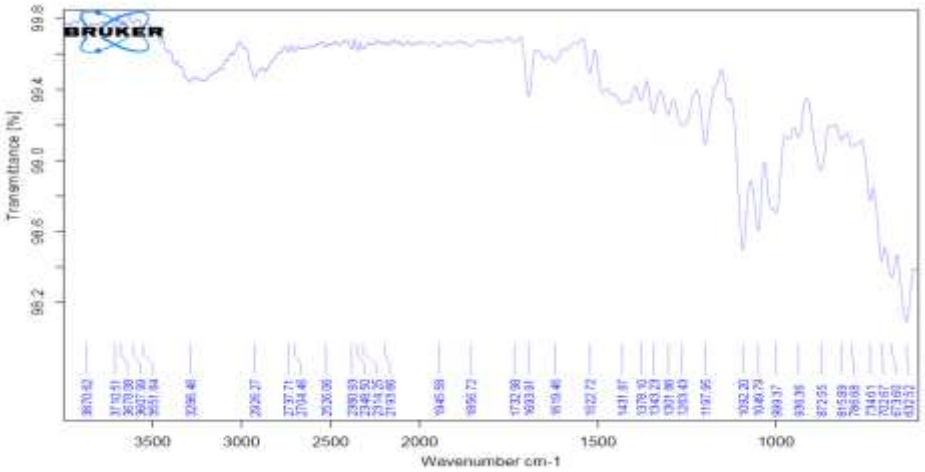

Figure 13: ATR spectrum of optimized formulation

Differential Scanning Calorimetry (DSC) study

It showed a sharp endothermal peak at 218.05 °C with heat of energy of -18.02 mJ; which is in agreement to the previous reports.

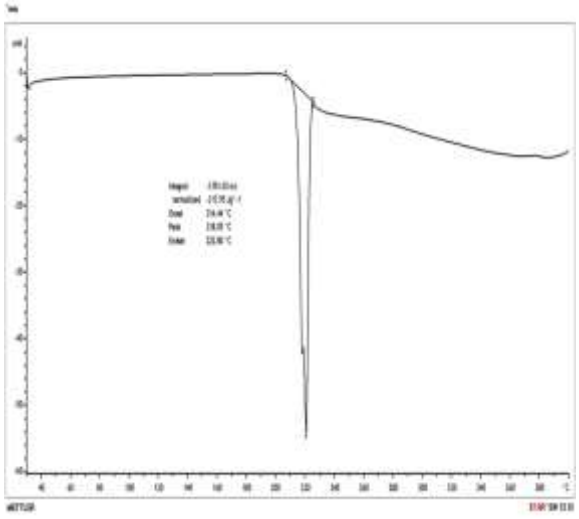

Figure 14: DSC thermo gram of the drug

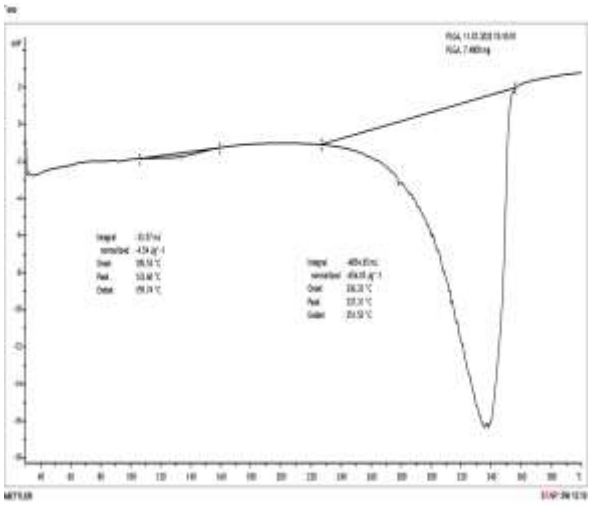

Figure 15: DSC thermo gram of PLGA

PLGA exhibited a characteristic peak at 337.31 which is as per the information available. DSC thermo gram of the drug exhibited an endothermal peak at 213.53 °C; which is near to the value of 218.105 as recorded earlier. This indicated no-interaction of the drug with

excipients. A narrow peak with small indicated uniform dispersion of doxorubicin and other excipients.

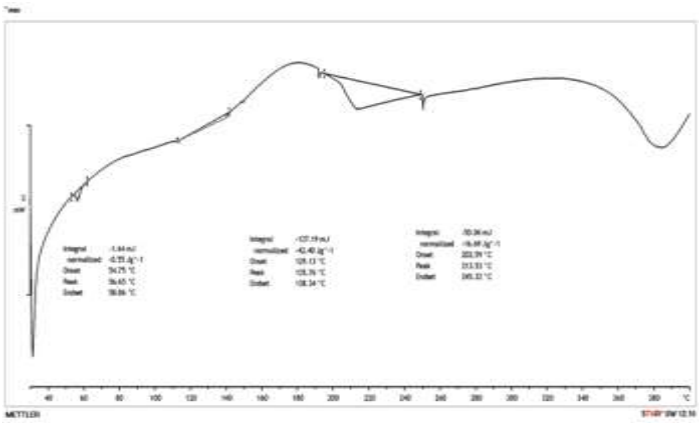

Figure 16: DSC thermo gram of optimized formulation

X Ray Diffraction (XRD) study

While analyzing the information, a lot of noise was observed which could be due to presence of moisture trapped during the isolation of the drug from crude extract. A broad peak at position 4 (2Theta) with intensity of 13000 was noted. Two more sharp peaks at position 12 and 16 (2Theta) with intensity below 5000 were also observed. Few more characteristic peaks appeared at 19, 22 (2Theta) and 30 (2Theta) with intensity below 2000.

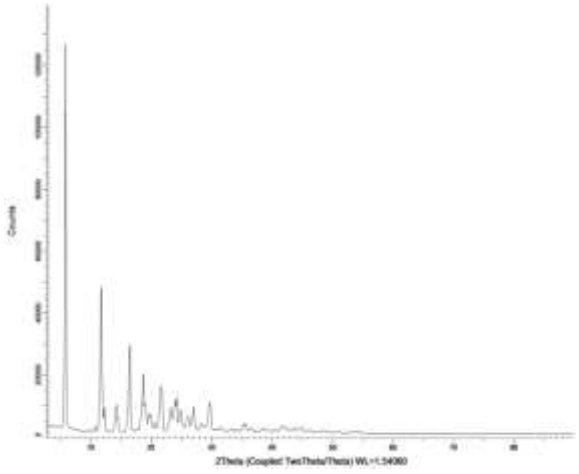

Figure 17: XRD spectrum of Doxorubicin

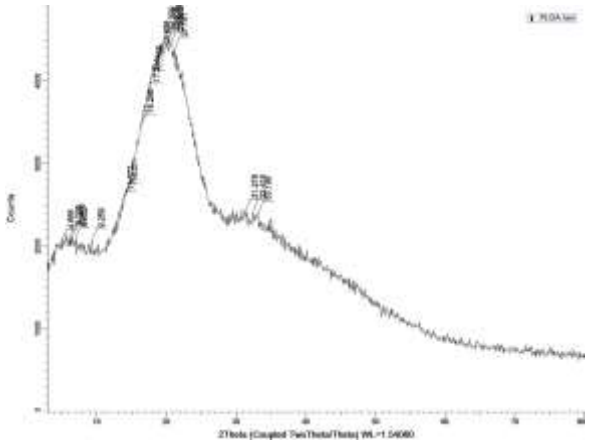

Figure 18: XRD spectrum of PLGA

PLGA was taken as the primary polymer in the nanoparticles in the current study. During the XRD study, peak position (2Theta) and intensity were observed. A characteristic intense and broad peak at position 20.81 (2Theta) with intensity of 500 was seen. Few more additional peaks were also observed at 6.07 (2Theta) and 32.418 (2Theta) with intensity below 300. However, the peaks were broad and numerous adjacent peaks were also developed which is possibly due to the moisture entrapment; as PLGA is hygroscopic in nature.

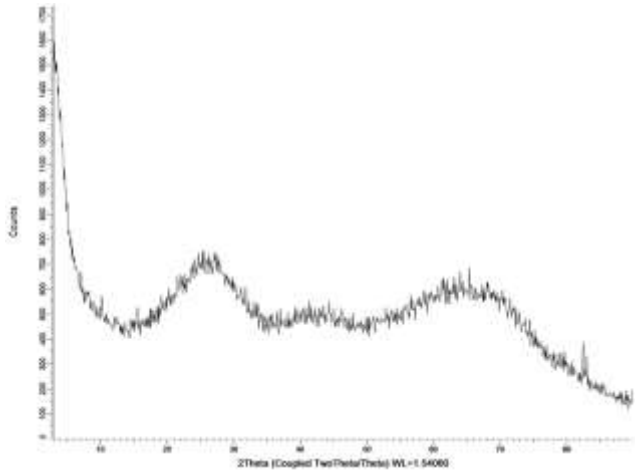

Figure 19: XRD spectrum of optimized nanoparticles

XRD study showed a significant characteristic peak at position 28.32, 42.15 and 65.38 (2Theta) with intensity of below 700. Additionally, few non-prominent peaks were also observed having intensity below 600. A large number of small and minor peaks was also observed which could be due to presence of solvent and reduced crystallinity. However, the peaks mentioned earlier were broad which could be due to the loss of crystallinity as well as finite disposition of drug crystal during nanoparticles preparation. It was also noted that, the peaks below 30 (2Theta) were obtained in case of doxorubicin only. The peak at 42.15 and 65.38 (2Theta) indicate crystalline arrangement of PLGA along with doxorubicin.

Surface morphology, particle size and zeta potential of optimized formulation

SEM study revealed that the optimized nanoparticles are spherical with smooth surface.

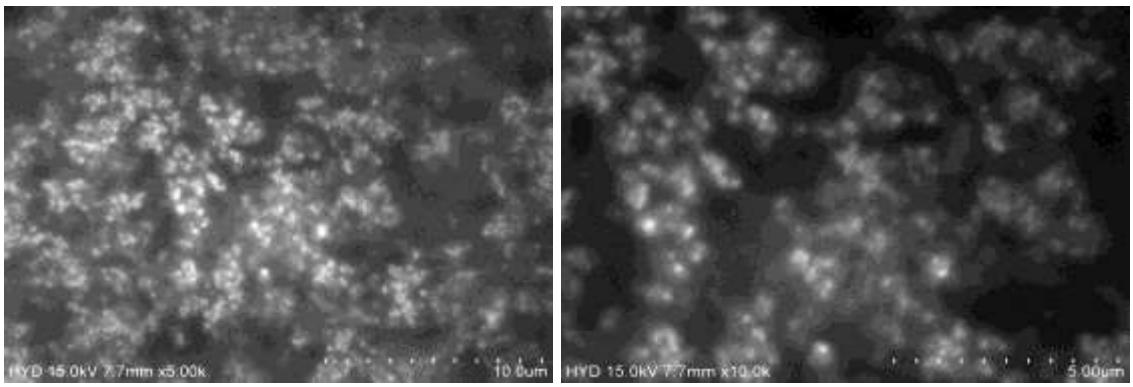

Figure 20: SEM photomicrograph of optimized formulation

The particle size study of optimized formulation revealed an average size of 282.6 nm. The polydispersity index (PI) was found to be 0.649.

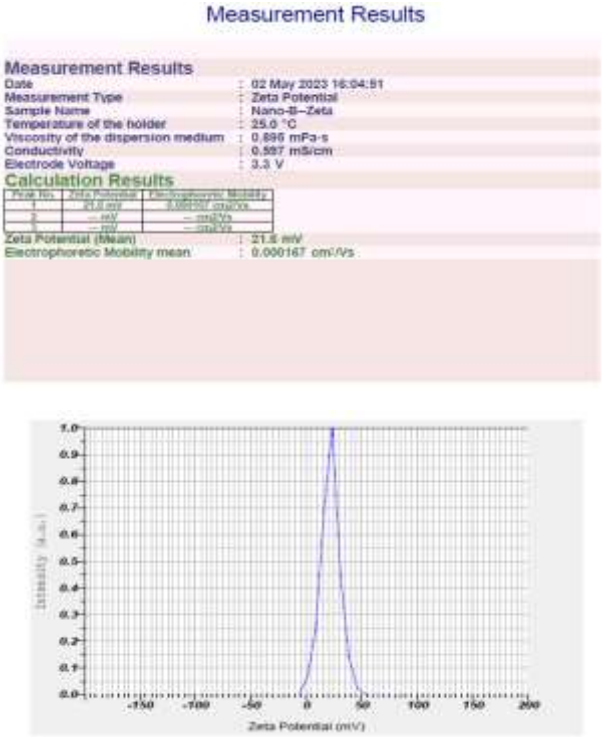

Figure 21: Zeta potential estimation of optimized formulation

The zeta potential of the nanoparticles dispersed in acetate buffer pH 4.0 was estimated and found to be 21.6 mV indicative of a stable dispersion.

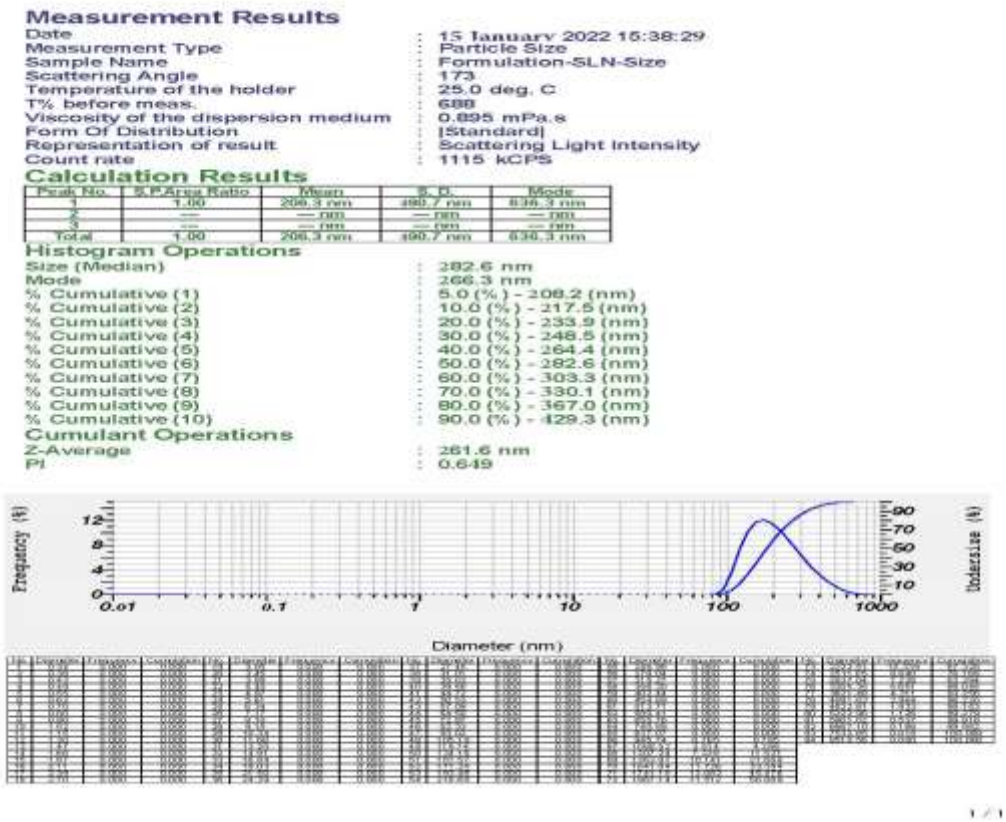

Figure 22: Particle size and size distribution of the optimized formulation

Cell morphological studies

The cell morphology changes in 0 h- and 24 h-treated groups were visualized using a CKX41 inverted microscope.

In vitro cell toxicity (Lactate Dehydrogenase Assay)

The cell-membrane damages of MCF-7 after treatment with different concentrations (1.25, 2.5, 5, 10, 20, 40, and 80 µg/ mL) of DOX NPs were measured by monitoring the release of LDH using CytoTox96 assay. The treated free DOX concentrations (0.1, 0.25, 0.5, 0.75, 1, 1.25, and 1.5 µg/mL) were measured using CytoTox96 assay, and the results are presented in Figure 23. The percent toxicity gradually increased with the concentration of as-prepared nanomaterials. As shown in figure 10, fewer cell toxicity effects were noted in DOX NPs treated cancer cells. The cell viability was noted to be more than 80% after incubation with the DOX NP for 24 h up to a concentration of 80 µg/mL. The cell toxicity study indicate that DOX NPs had significantly higher toxicity. The higher cell toxicity effect of DOX NPs may be attributed to receptor-mediated endocytosis by MCF-7 cells, which increases the drug concentration in the intracellular environment.

Table 7: Cell toxicity of MCF-7 cell lines after being treated with different concentrations of DOX (1.25-80 µg/ml)

DOX Concentration (µg/ml)	**Cytotoxicity (%)**				
				Mean	**SD**
0	0	0	0	0	0
1.25	3	2.56	3.44	3	0.44
2.5	21	18.56	23.56	21.04	2.50
5	23	25.89	23.56	24.15	1.53
10	27	31.23	29.84	29.35	2.15
20	36	38.55	35.21	36.58	1.74
40	68	62.56	69.21	66.59	3.54
60	82	85.23	78.56	81.93	3.33
80	97	98.56	95.61	97.05	1.47

***In vitro* morphological analysis.**

In vitro morphological changes of MCF-7 cells were observed by inverted light microscopy, and the results are given in Figure 23. A drastic change in the morphology of the MCF-7 cells

was noted after 24 h treatment. The Dox NPs treated MCF-7 cells displayed intrinsic damage and shrinkages as compared to the control group. The use of Dox NPs caused more cell destruction, while in the case of Dox NPs, the cell line showed smaller morphology changes than those treated with free DOX alone.

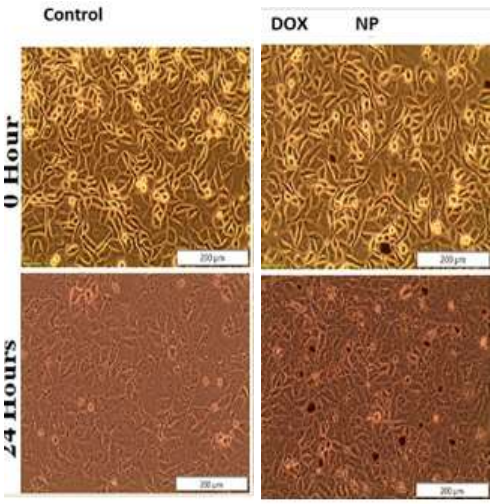

Figure 23: In vitro morphological changes

Conclusion

Doxorubicin PLGA NPs were designed and developed by Design-Expert® Software. The NPs were prepared using the double emulsification and precipitation method. Three independent factors such as concentration of PLGA 50:50 (A), PVA (B), stirring speed (C) were considered. ATR and DSC studies indicated that there was no interaction between the drug and polymers. The morphological studies performed by SEM showed uniform and spherical shaped discrete particles with smooth surface having the size of 282.6 nm. X-ray diffraction was performed to confirm the crystalline nature of the drug after encapsulation. The NPs exhibited a zeta potential of 21.6 mV. *In vitro* release studies showed drug release up to 10 hrs. The release kinetics study indicated first order release. The cell viability was found to be more than 80% after incubation with the Dox NPs for 24 h up to a concentration of 80 µg/ml. The Dox NPs treated MCF-7 cells displayed intrinsic damage and shrinkages as compared to the control group. It may be concluded from the present investigation that PLGA NPs of Doxorubicin can effectively treat the breast cancer.

REFERENCES

1. Pieper S, Onafuye H, Mulac D, Cinatl J Jr, Wass MN, Michaelis M, Langer K. Incorporation of doxorubicin in different polymer nanoparticles and their anticancer activity. Beilstein J Nanotechnol. 2019 Oct 29; 10:2062-2072.
2. Firouzi Amoodizaj F, Baghaeifar S, Taheri E, Farhoudi Sefidan Jadid M, Safi M, Seyyed Sani N, Hajazimian S, Isazadeh A, Shanehbandi D. Enhanced anticancer

potency of doxorubicin in combination with curcumin in gastric adenocarcinoma. Journal of Biochemical and Molecular Toxicology. 2020 Jun;34(6): e22486.

3. Ashrafizadeh M, Mirzaei S, Gholami MH, Hashemi F, Zabolian A, Raei M, et al. Hyaluronic acid-based nanoplatforms for Doxorubicin: A review of stimuli-responsive carriers, co-delivery and resistance suppression. Carbohydrate Polymers. 2021;272:118491.
4. Yang F, Teves SS, Kemp CJ, Henikoff S. Doxorubicin, DNA torsion, and chromatin dynamics. Biochim Biophys Acta. 2014;1845(1):84-9.
5. Varela-López A, Battino M, Navarro-Hortal MD, Giampieri F, ForbesHernández TY, Romero-Márquez JM, et al. An update on the mechanisms related to cell death and toxicity of doxorubicin and the protective role of nutrients. Food Chem Toxicol. 2019; 134:110834.
6. Thorn CF, Oshiro C, Marsh S, Hernandez-Boussard T, McLeod H, Klein TE, et al. Doxorubicin pathways: Pharmacodynamics and adverse effects. Pharmacogenet Genomics. 2011;21(7):440–46.
7. Ruggiero A, De Rosa G, Rizzo D, Leo A, Maurizi P, De Nisco A, et al. Myocardial performance index and biochemical markers for early detection of doxorubicin-induced cardiotoxicity in children with acute lymphoblastic leukaemia. Int J Clin Oncol. 2013;18(5):927-33.
8. Marina NM, Cochrane D, Harney E, Zomorodi K, Blaney S, Winick N, et al. Dose escalation and pharmacokinetics of pegylated liposomal Doxorubicin (Doxil) in children with solid tumors: A pediatric oncology group study. Clin Cancer Res. 2002;8(2):413-8
9. Hasanain Gomhor J Alqaraghuli, Soheila Kashanian, Ronak Rafipour,2019, A review on targeting nanoparticles for breast cancer, Current pharmaceutical biotechnology, 20 (13) , 21-53.
10. Lim, E. K., Chung, B. H., and Chung, S. J. (2018). Recent advances in pH-sensitive polymeric nanoparticles for smart drug delivery in cancer therapy. Curr. Drug Targets 19, 300–317. doi: 10.2174/1389450117666160602202339
11. Jain, R. K. (1994). Barriers to drug delivery in solid tumors. Sci. Am. 271, 58–65. doi: 10.1038/scientificamerican0794-58
12. Cagel, M., Tesan, F. C., Bernabeu, E., Salgueiro, M. J., Zubillaga, M. B., Moretton, M. A., et al. (2017). Polymeric mixed micelles as nanomedicines: achievements and perspectives. Eur. J. Pharm. Biopharm. 113, 211–228.

13. Shi, J., Xiao, Z., Kamaly, N., and Farokhzad, O. C. (2011). Self-assembled targeted nanoparticles: evolution of technologies and bench to bedside translation. ACC Chem. Res. 44, 1123–1134. doi: 10.1021/ar200054n
14. Farokhzad, O. C., and Langer, R. (2009). Impact of nanotechnology on drug delivery. ACS Nano 3, 16–20. doi: 10.1021/nn900002m
15. Acharya, S., and Sahoo, S. K. (2011). PLGA nanoparticles containing various anticancer agents and tumour delivery by EPR effect. Adv. Drug Deliv. Rev. 63, 170–183. doi: 10.1016/j.addr.2010.10.008
16. Peng, X. Liang. Progress in research on gold nanoparticles in cancer management. Medicine 98: 234-39 (2019).
17. Ales Sorf, Dimitrios Vagiannis, Fahda Ahmed, Jakub Hofman, Martina Ceckova, Dabrafenib inhibits ABCG2 and cytochrome P450 isoenzymes; potential implications for combination anticancer therapy, Toxicology and Applied Pharmacology, 10.1016/j.taap.2021.115797, 434, (115797), (2022).
18. S. Goodall, M.L. Jones, and S. Mahler. Monoclonal antibody- targeted polymeric nanoparticles for cancer therapy–future prospects. Journal of Chemical Technology & Biotechnology 90: 1169-76 (2015).
19. Pardeike, J., Hommoss, A., Müller, R.H. Lipid nanoparticles (SLN, NLC) in cosmetic and pharmaceutical dermal products. Int. J. Pharm. 2009, 366, 170–184.
20. Naseri, N.; Valizadeh, H.; Zakeri-Milani, P. Solid lipid nanoparticles and nanostructured lipid carriers: Structure, preparation and application. Adv. Pharmaceut. Bull. 2015, 5, 305.
21. Shirodkar, R.K.; Kumar, L.; Mutalik, S.; Lewis, S. Solid lipid nanoparticles and nanostructured lipid carriers: Emerging lipid based drug delivery systems. Pharm. Chem. J. 2019, 53, 440–453.
22. Carvalho, P.M.; Felício, M.R.; Santos, N.C.; Gonçalves, S.; Domingues, M.M. Application of light scattering techniques to nanoparticle characterization and development. Front. Chem. 2018, 6, 237.
23. Ud Din, F.; Aman, W.; Ullah, I.; Qureshi, O.S.; Mustapha, O.; Shafique, S.; Zeb, A. Effective use of nanocarriers as drug delivery systems for the treatment of selected tumors. Int. J. Nanomed. 2017, 12, 7291.
24. Bayón-Cordero, L.; Alkorta, I.; Arana, L. Application of solid lipid nanoparticles to improve the efficiency of anticancer drugs. Nanomaterials 2019, 9, 474.

25. Sivakumar, S. Therapeutic potential of chitosan nanoparticles as antibiotic delivery system: Challenges to treat multiple drug resistance. Asian J. Pharm. Free Full Text Artic. Asian J. Pharm 2016, 10, 2.
26. Keizer HG, Pinedo HM, Schuurhuis GJ, Joenje H. Doxorubicin (adriamycin): A critical review of free radical-dependent mechanisms of cytotoxicity. Pharmacol Ther. 1990;47(2):219-31.
27. Renu K, Abilash VG, Pichiah TPB, Arunachalam S. Molecular mechanism of doxorubicin-induced cardiomyopathy – an update. Eur J Pharmacol. 2018; 818:241–53.
28. Minotti G, Menna P, Salvatorelli E, Cairo G, Gianni L. Anthracyclines: Molecular advances and pharmacologic developments in antitumor activity and cardiotoxicity. Pharmacol Rev. 2004;56(2):185-229.
29. Meredith AM, Dass CR. Increasing role of the cancer chemotherapeutic doxorubicin in cellular metabolism. J Pharm Pharmacol. 2016;68(6):729- 41.
30. Sonowal H, Pal PB, Wen JJ, Awasthi S, Ramana KV, Srivastava SK. Aldose reductase inhibitor increases doxorubicin-sensitivity of colon cancer cells and decreases cardiotoxicity. Sci Rep. 2017;7(1):3182.
31. Shi Y, Bieerkehazhi S, Ma H. Next-generation proteasome inhibitor oprozomib enhances sensitivity to doxorubicin in triple-negative breast cancer cells. Int J Clin Exp Pathol. 2018;11(5):2347–55.